Rapid construction of a patient-specific torso model from 3D ultrasound for non-invasive imaging of cardiac electrophysiology

L. K. Cheng[1] G. B. Sands[1] R. L. French[2] S. J. Withy[2]
S. P. Wong[3] M. E. Legget[2] W. M. Smith[2] A. J. Pullan[1]

[1]Bioengineering Institute, The University of Auckland, New Zealand
[2]Auckland City Hospital, Auckland, New Zealand
[3]Middlemore Hospital, Auckland, New Zealand

Abstract—*One of the main limitations in using inverse methods for non-invasively imaging cardiac electrical activity in a clinical setting is the difficulty in readily obtaining high-quality data sets to reconstruct accurately a patient-specific geometric model of the heart and torso. This issue was addressed by investigation into the feasibility of using a pseudo-3D ultrasound system and a hand-held laser scanner to reconstruct such a model. This information was collected in under 20 min prior to a catheter ablation or pacemaker study in the electrophysiology laboratory. Using the models created from these data, different activation field maps were computed using several different inverse methods. These were independently validated by comparison of the earliest site of activation with the physical location of the pacing electrodes, as determined from orthogonal fluoroscopy images. With an estimated average geometric error of approximately 8 mm, it was also possible to reconstruct the site of initial activation to within 17.3 mm and obtain a quantitatively realistic activation sequence. The study demonstrates that it is possible rapidly to construct a geometric model that can then be used non-invasively to reconstruct an activation field map of the heart.*

Keywords—*Model construction, Geometric model, 3D ultrasound, Validation, Inverse problem, Human heart*

Med. Biol. Eng. Comput., 2005, **43**, 325–330

1 Introduction

SINCE THE initial conception of the ECG (WALLER, 1887) and the later development of the standard 12-lead ECG (GOLDBERGER, 1942), there have been relatively few advances in the field of non-invasive electrocardiography. The well-known 12-lead ECG is still the standard method used for the initial diagnosis and monitoring of cardiac function. However, its use is subject to interpretation by the clinician.

The concept of using mathematical modelling, inverse algorithms and a larger lead set to unravel the attenuation effects of the body surrounding the heart has been studied for many years (BARR and SPACH, 1978). However, despite continued research into this topic (RAMANATHAN *et al.*, 2004; CHENG *et al.*, 2003*a*; OSTER *et al.*, 1997; MESSINGER-RAPPORT and RUDY, 1988), inverse algorithms are still not routinely used in a clinical setting. One of the reasons for this is the relatively large amount of additional information required by an inverse algorithm compared with a standard 12-lead ECG, in particular the geometry and relative positions of the heart and torso and the locations of the torso surface recording electrodes, as well as a relatively large number of high-quality potential recordings. Obtaining this range of information can often take a significant amount of time, especially if different imaging modalities need to be used to gather the varying types of information.

The accuracy of the geometric model is known to be the single greatest determinant of the final accuracy of a computed inverse solution (CHENG *et al.*, 2003*b*). From this extensive simulation study, it was found that torso size and shape and the size and position of the heart within the torso had the largest influences on the accuracy of the inverse solution. It is therefore essential in any model-based inverse analysis to obtain accurate descriptions of these regions.

Traditionally, geometric models used for non-invasive imaging of cardiac excitation have been constructed from magnetic resonance (MR) or computed tomography (CT) images (MODRE *et al.*, 2002; PULLAN *et al.*, 2001; RAMANATHAN *et al.*, 2004). However, both of these techniques may be inappropriate for routine clinical use. With MRI, the typically lengthy time required for a full torso scan is detrimental to obtaining solutions rapidly, and, with CT, the exposure to radiation is of concern. In our experience in New Zealand and the United Kingdom, access to CT and MRI facilities,

Correspondence should be addressed to Dr Leo K. Cheng; email: l.cheng@auckland.ac.nz

Paper received 27 July 2004 and in final form 17 November 2004
MBEC online number: 20054000

even in modern hospitals, can be difficult to obtain, as these facilities are typically in high demand. Recently, a method using fluoroscopy and stereovision has also been developed as an alternative to CT and MRI (GHANEM *et al.*, 2003). However, this technique is only able to indicate the overall extent of the epicardial surface rather than the myocardial geometry itself.

In this work, we investigate the use of a standard cardiac ultrasound machine to obtain heart geometry and the use of a hand-held laser scanner to obtain external geometries. Compared with MRI, such imaging modalities can greatly reduce the time associated with collecting the geometric data required for an inverse analysis, with less than 20 min required to obtain sufficient information. We expect that the geometric errors associated with the models constructed from these imaging modalities will be larger when compared with errors in models constructed from MRI or CT, owing to the non-uniformity and sparsity of the data. However, despite this additional error, the removal of the dependence on MRI or CT will eliminate what is currently a significant hurdle in routinely and rapidly constructing patient-specific models.

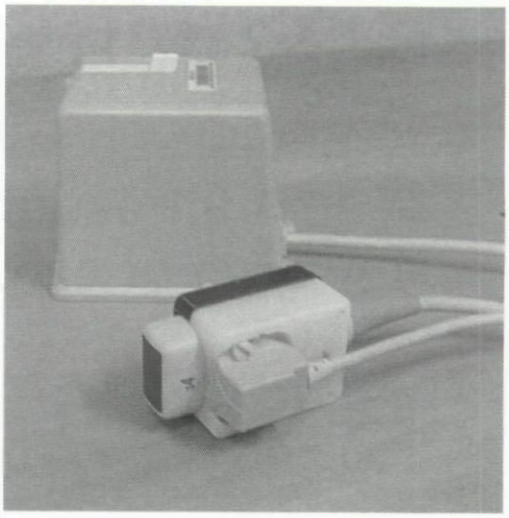

Fig. 1 *Standard cardiac ultrasound probe with magnetic tracker (foreground) attached by custom-moulded holder to track position and orientation in space. Magnetic reference transmitter is shown in background*

2 Model construction

2.1 *Heart model*

The patient-specific ventricular geometry was obtained using a pseudo-three-dimensional ultrasound set-up (LEGGET *et al.*, 1998). It requires attachment of a Flock of Birds (6D-FOB) magnetic tracking device* to a standard cardiac ultrasound probe, as shown in Fig. 1. By tracking the strengths and orientations of the magnetic field gradients (generated by an associated magnetic field transmitter), it is possible to reconstruct the location and orientation of the ultrasound probe, and thus each ultrasound image can be precisely positioned in three-dimensional space.

The ultrasound images were obtained using a standard ultrasound machine† with a 4 MHz phased array transducer. The imaging was performed on a non-metallic bed with the subject in a supine position: the same position from which all electrical recordings were obtained. Images were acquired during 6 s breath-holding sequences to reduce the effects of respiratory motion artifact. A concurrent ECG signal was also obtained to gate the ultrasound image acquisition to the point of maximum inflation of the cardiac cycle. Images of the valve planes and the ventricles were obtained from approximately ten different views for each subject. The depth of the ultrasound view was set to obtain maximum coverage of the heart and could be varied for each view, but typically remained constant for each subject.

Landmark positions at key points on the torso surface (e.g. shoulders, hips, xiphoid process and sternal notch) were also obtained by placing the ultrasound probe on each of these locations. The positions of these landmarks were acquired at the beginning and the end of the ultrasound scanning sequence to determine the amount of movement during the image acquisition process and to align the dataset with other imaging modalities used in this study. The table plane was also used as an additional reference to define the back of the torso model. From these ultrasound image sequences, the frames immediately following the QRS-complex but prior to contraction (i.e. at end-diastole) were extracted and used to digitise the ventricular surfaces as well as features such as the mitral, tricuspid and aortic valves and the ventricular apex (used to position an initial ventricular heart model in the correct orientation). An example of a digitised ultrasound image with endocardial and epicardial surfaces identified is shown in Fig. 2.

The quality and distribution of the digitised ultrasound data vary from subject to subject owing to the acoustic visibility of the heart through the rib cage and the position of the lungs. Depending on the quality of the data obtained from the ultrasound images, it is possible to create the heart model using either a traditional least squares fitting technique (BRADLEY *et al.*, 1997) or using a non-linear host mesh fitting technique (NASH *et al.*, 2000; SCHULTE *et al.*, 2001).

The least squares fitting method is formulated as a problem that minimises the distance between digitised data points and orthogonal points on the geometric mesh. This can be expressed as

$$\min F(u) = \sum_{d=1}^{D} (u(\xi_d) - u_d)^2 \tag{1}$$

where d is a given data point, D is the total number of data points, u_d is the position of the data point, and $u(\xi_d)$ is the location of the orthogonal projection of that data point onto the surface of the geometric model.

The host mesh fitting technique deforms an existing model to match subject-specific data, allowing the topology of the generic mesh to be maintained even in regions where there

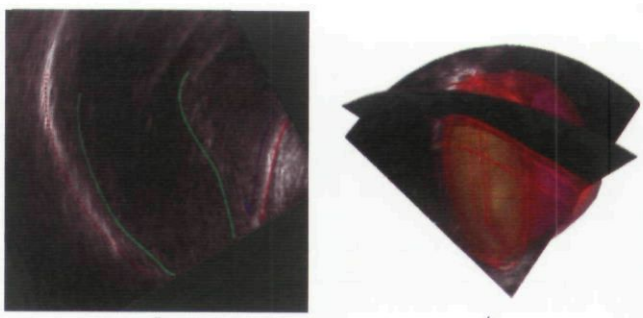

a b

Fig. 2 *Patient-specific three-dimensional heart model created from two-dimensional ultrasound images. (a) Digitisation of left and right endocardial and epicardial surfaces from two-dimensional ultrasound image; (b) final ventricular heart mesh with two of ultrasound images used to create this model overlaid*

*Flock of Birds, 2002, Ascension Technology Corporation, Burlington, VT; http://www.ascension-tech.com/products/flockofbirds.php
†Sonos 5500, Hewlett-Packard

are few data present (e.g. the right ventricular free wall, which is a difficult region of the heart to image using ultrasound), while accurately matching regions where data are present.

The generic heart mesh used here had been previously created from detailed multiple-plane MRI images of a healthy 28 year old male subject. These images were ECG gated in end-diastolic state and digitised. They were then fitted with bicubic Hermite elements using a traditional least-squares fitting technique (BRADLEY *et al.*, 1997) with a final RMS error of 2.4 mm. The host mesh fitting process has been used previously to customise hearts of known geometry and validated against MRI data with both animal (sheep) and human hearts, showing surface errors of less than 3 mm RMS (SCHULTE *et al.*, 2001).

2.2 *Torso surface model and potential recordings*

Electrical potential recordings were simultaneously obtained from 256 electrode locations using a commercial mapping system[‡], with a sampling frequency of 1 kHz. Carbon electrodes, which are translucent to fluoroscopy, were embedded within an elastic jacket (as shown in Fig. 3*a*) and connected to the recording system using carbon wires and electrode clips. Approximately 144 of the electrodes were attached on the anterior, and 112 were attached on the posterior. The torso surface was prepared by being wiped with alcohol and, if necessary, by being shaved. Conductive gel was also placed on each electrode to reduce the surface impedance.

The external torso geometry and the locations of all the recording electrodes were also required for the inverse procedure. To obtain this information a hand-held laser scanner** was used. The laser scanner (shown in Fig. 3*b*) samples points on three-dimensional surfaces using a wand, the orientation and position of which are determined by an embedded magnetic tracking system. The wand contains a laser that generates a bright line on a surface, and the three-dimensional positions of points on that line are reconstructed using standard stereographic techniques. The white spots on the jacket indicate the tips of the electrodes and can be easily detected by the reflected laser light, whereas black surfaces do not reflect the laser light and are ignored by the scanner. Additional markers were also placed on a number of electrodes and used as landmarks to allow the laser data to be registered to the ultrasound and fluoroscopic images. The scanning information was gathered in under 5 min, during breath-holding sequences in the electrophysiology laboratory prior to the commencement of the study.

3 Catheter localisation

A heart that is being paced from a known location (such as with a pacemaker or a catheter) mimics an ectopic focus and, as such, generates a well-defined activation sequence. For our studies, volunteer subjects either had previously received an implanted pacemaker or were undergoing catheter ablation surgery. In both these situations, the ventricle was paced from a fixed location. Written informed consent was obtained from each subject, and experiments were approved by the Auckland Ethics Committee.

The location of the pacing catheter was reconstructed from fluoroscopic images. As biplanar X-ray was not present in the electrophysiology laboratory, two orthogonal single-plane images were used at left anterior oblique (LAO) 45° and right anterior oblique (RAO) 45°. Fluoroscopic image sequences of 3 s duration were obtained during breath-holding and then gated against ECG recordings to identify the diastolic state. Lead spheres, 1 mm in diameter, were also placed on a number of body surface electrodes and used to align the fluoroscopic images with the locations of the electrodes determined by the laser scanner, as shown in Fig. 4. The fluoroscopic images were corrected for non-linear geometric distortions (e.g. pincushion, barrel, interactions with external magnetic fields) through the use of a phantom grid (ONNASCH and PRAUSE, 1992). Grid distortion was computed using a 'snake' active contouring (KASS *et al.*, 1987) algorithm. The grid intersections were fitted to a finite element deformation field to give a calibration matrix from which the undistorted fluoroscopic images were computed. Biplanar registration was achieved by imaging a three-dimensional phantom (with 48 lead spheres) from two orthogonal views. The stereographic views were then used to reconstruct common points in three-dimensional space (GHANEM *et al.*, 2003).

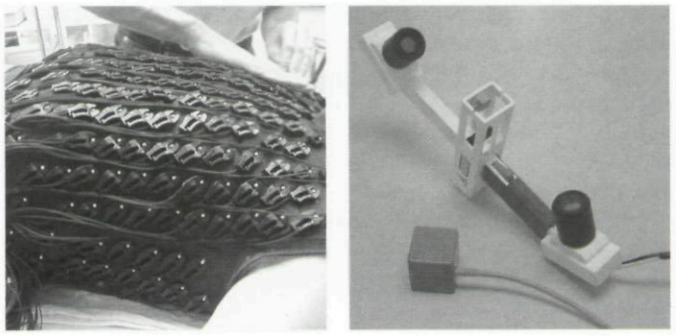

a *b*

Fig. 3 *(a) Elastic jacket embedded with 256 electrodes. Each carbon clip attaches to recording electrode marked by white spot and carries recorded signal to mapping system. Locations of each electrode were determined by (b) hand laser scanner with recording cameras at each end of wand used to detect the laser emitted from centre of wand*

4 Validation results

We present here results from our first complete patient study illustrating the feasibility of using our rapidly constructed geometric model for non-invasively determining the electrical activity at the heart level. The results were computed using inverse algorithms that determine either myocardial activation time or epicardial potential solutions (CHENG *et al.*, 2003*a*). The site of initial activation, as specified by these reconstructed

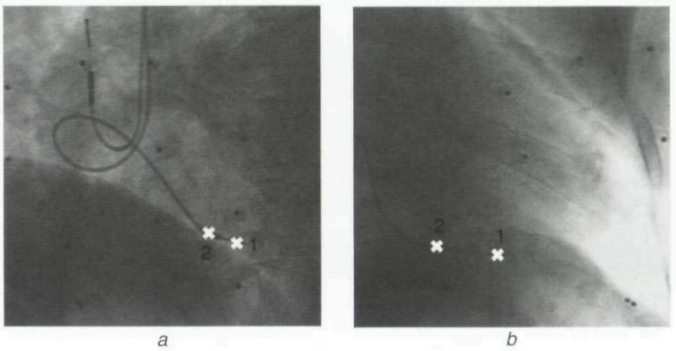

a *b*

Fig. 4 *Two fluoroscopic views of pacemaker wires at same point in cardiac cycle. The (1) Cathode pacing tip and (2) anode ring have been marked with crosses. Dark spheres show locations of lead balls placed on recording electrodes used to register with other imaging modalities*

[‡]UnEmap, 2002, The University of Auckland; http://www.unemap.com

**FastSCAN, 2002, Polhemus Incorporated; http://www.polhemus.com/fastscantech.htm

solutions, was directly compared with the known site of the pacing electrode within the right ventricle. We include a brief summary of the activation and potential-based methods used non-invasively to reconstruct the ventricular electrical activity below; however, further details can be found in HUISKAMP and GREENSITE (1997) and GREENSITE and HUISKAMP (1998).

The potential-based inverse method (GREENSITE and HUISKAMP, 1998) formulation is given by

$$\phi_H(y, t) = \boldsymbol{A}^{\dagger}_{\lambda_i}[\phi_B(x, t)] \tag{2}$$

where y represents a location on the epicardial surface, x represents a location on the body surface, t is a given time step, ϕ_H are the reconstructed epicardial potentials, ϕ_B are the measured body surface potentials, and $\boldsymbol{A}^{\dagger}_{\lambda_i}$ is the regularised epicardial to body surface transfer matrix, with the regularisation parameter λ_i for a given equation i determined using either the L-curve (HANSEN and O'LEARY, 1993) or zero-crossing methods (JOHNSTON and GULRAJANI, 1997).

The activation-based inverse method involves minimising the difference between the measured body surface potentials and those predicted by a given activation field. The objective function that was minimised is given in

$$\tau(y) = \min \|(\boldsymbol{A}\phi_M - \phi_B)\|_2 + \|\lambda \boldsymbol{L}\tau(y)\|_2 \tag{3}$$

where $\tau(y)$ is the activation time of a point y on the heart, ϕ_B is as defined in (2), ϕ_M is the transmembrane potential, $\boldsymbol{A}$ is a transfer matrix that maps transmembrane potentials to body surface potentials, and λ is a parameter that scales the weighting of the surface Laplacian $\boldsymbol{L}$ of the activation field.

In the study presented here, recordings were obtained for 10 s durations from a total of 256 electrodes, of which 48 channels were rejected owing to poor electrode contact. The ventricular surfaces were constructed from 13 ultrasound image planes and fitted using the host mesh fitting process described in Section 2.1. The epicardial and endocardial surfaces each had 262 nodes and 280 elements. All of the ventricular surfaces were comprised of bicubic Hermite elements. The final RMS error between the digitised points and the fitted surfaces was 3.0 mm.

The torso surface mesh consisted of 1034 nodes and 1056 bicubic Hermite elements. The torso surface was fitted to the electrode positions determined by the hand laser scanner using a standard fitting process to an average RMS error of 9.8 mm. This relatively large error in the torso surface reconstruction was due to a lack of data acquired by the laser scanner near the hips of this subject, and most of the largest error residuals were located in this unimportant region.

The pacemaker used in our study was a DR1276[††], with a pacesetter 1470T lead. The distance between the tip cathode (lower sphere, Fig. 5) and ring anode (top sphere in Fig. 5) was 29 mm. This distance was reconstructed to be 27.3 mm from the fluoroscopy images. This provides an indication of the accuracy of the location of the pacing electrode.

A comparison between two of the solutions and the site of initial pacing is given in Fig. 5. Activation maps show the site of initial activation as the red region and points of late activation as blue regions. Fig. 5*a* shows the activation pattern on the epicardial and endocardial surfaces, as reconstructed by the myocardial activation inverse algorithm (HUISKAMP and GREENSITE, 1997), and, in Fig. 5*b*, is the epicardial activation pattern derived from an epicardial potential inverse algorithm (GREENSITE and HUISKAMP, 1998), with the regularisation

[††]Guidant Meridian

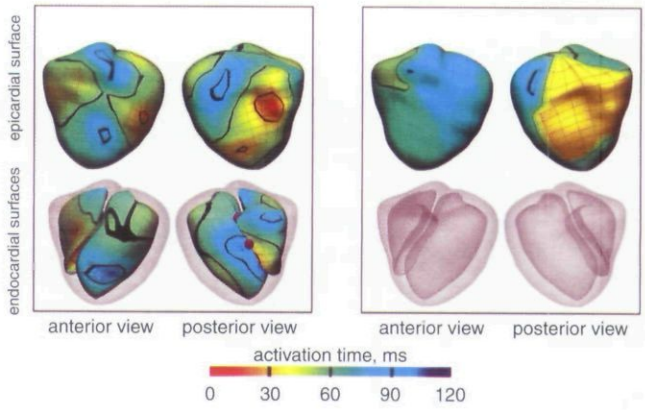

Fig. 5 *Comparison of activation maps (red = early activation; blue = late activation) produced by inverse algorithms on anterior and posterior views of heart. (a) Activation inverse method; (b) Greensite potential inverse method. Two purple spheres represent cathode (lower) and anode (upper and partially obscured) electrodes of pacing wires located near septum. Top shows solution on epicardial surface. Bottom shows solution on endocardial surfaces, with transparent epicardial surface. For potential-based inverse solution, there is no valid solution on endocardial surface*

parameters determined using the L-curve method. The epicardial potential solution has been converted to activation times by assigning the activation time to be the time of greatest negative slope of the epicardial potential signal trace, as determined by a moving finite difference window (CHENG *et al.*, 2003*a*).

The initial site of activation, as determined by the activation inverse solution, can be directly compared with locations of the pacemaker electrodes shown in Fig. 5*a*, as reconstructed from the fluoroscopic sequences. The pacing electrodes are illustrated, with the lower sphere being the cathode and the upper sphere being the ring anode. The difference between the site of initial activation as determined by the activation inverse solution and the cathode electrode was 17.3 mm. There was a significant difference between the solutions produced by the epicardial potential and the activation inverse methods. The difference in the activation maps between the epicardial inverse solutions and the activation inverse solutions (only comparing the solutions at all of the 262 nodes on the epicardial surfaces) was 18.7 ms RMS. However, it should be noted that the epicardial inverse solutions have an inherent disadvantage, as the site of initial activation is known to occur on the endocardial surface.

Overall, the results are consistent with those presented by MESSNARZ *et al.* (2004), which showed, using simulated and clinical data (when using models constructed from MRI), that activation inverses were more robust and stable than the potential-based methods. However, even with the differences in potential and activation inverse methods, our results both have early activation on the posterior right epicardial surface and latest activation on the anterior surface. The earliest site of activation on the epicardial surface is closest to the catheter electrodes and mimics the endocardial surfaces to some degree. This is similar in trend to results presented in previous studies (CHENG *et al.*, 2003*a*).

When the different potential-based methods were compared with each other, their solutions were all highly correlated (average RMS difference of 8.4 ms), regardless of the inverse algorithm used (Tikhonov, Greensite) or the method used to determine the regularisation parameter (L-curve or zero crossing).

5 Discussion

We have presented results from a pilot study that investigated the use of ultrasound to construct patient-specific models for use in inverse analysis. At this stage, we have successfully applied this only to a single patient, which limits the conclusions that can be drawn. However, the results do indicate that it may be possible to obtain a qualitatively realistic inverse solution using a geometric model that has been constructed using inexpensive, fast and readily available imaging methods, such as ultrasound and a hand-held laser scanner. Our methods also allowed fast acquisition of the data required to generate the geometric model (less than 20 min), with the ultrasound obtained on the morning of the study, and laser scanning obtained in the electrophysiology laboratory immediately prior to the pacemaker study.

In our study, the site of initial activation as reconstructed by the inverse algorithm was determined to be within 17.3 mm of the cathode electrode of the pacing wire. This solution is in the range of previous studies that have localised pacing tips from body surface potential maps to an accuracy of 20–25 mm (PESOLA *et al.*, 1999; SIPPENSGROENEWEGEN *et al.*, 1993). Using magnetic fields, the reported localisation accuracies were in the range of 5–30 mm (PESOLA *et al.*, 1999). However, in each of these cases, the geometric models were reconstructed from MRI images. We have shown that, despite our larger geometric errors resulting from the non-uniform and sparse data compared with those created from MRI data, our inverse solution is in a similar range to those constructed with a more accurate geometric model.

There exist a number of different sources of error that accumulate during the construction of the geometric model. From our own phantom studies and others, the anatomical location of a point in the ultrasound images can be determined with an accuracy of less than 2 mm (LEGGET *et al.*, 1998). This is significantly more accurate than the 10 mm accuracy reported in the study using fluoroscopy images (GHANEM *et al.*, 2003). Our studies have also shown that the site of the pacing catheter can be localised with errors of less than 3 mm from fluoroscopic images. Geometry from the laser scanner can be obtained within 2 mm under typical conditions. However, additional errors also arise from converting these raw data into the computational model. Taking all these factors into account, we believe there is an average error in the geometric model of around 5–10 mm.

The definitive site of initial activation owing to the pacemaker pulse is also unclear. We have compared our inverse solutions with the cathode tip of the pacing wire. However, it has also been shown that the site of initial activation can occur away from the cathode (LU *et al.*, 1992). It has been shown that factors such as anode ring surface area and pacing wire stiffness can cause the site of initial pacing to occur at the anode ring.

Our study has shown that it is feasible to obtain the necessary geometric data in a clinical setting without the use of MRI or CT. Despite the uncertainties involved in combining our various imaging modalities, the overall error in our inverse solutions is well within the range reported using models constructed using the more accurate MRI and CT. The modalities used to construct our model are all relatively cheap and readily available, and the short time required to obtain such data allows patient-specific models to be constructed on a routine basis. The results obtained are possibly not accurate enough for clinical use at this stage; however, it appears that one of the main hurdles of reliance on MRI or CT for model reconstruction may be overcome through the use of our methods. We are currently further quantifying the accuracy of the heart meshes constructed from three-dimensional ultrasound by comparing them directly with models constructed from MR images of the same patients, and we intend to validate our inverse methods by performing subsequent studies upon humans.

Acknowledgments—The authors would like gratefully to acknowledge the support of the theatre staff and other associated personnel at Green Lane Hospital. The authors also gratefully acknowledge the support of Professor Florence Sheehan and Dr Ed Bolson from the Cardiac Imaging Laboratory, University of Washington, Seattle, in establishing the 3D echo system at Green Lane Hospital.

The three-dimensional echocardiography system was established with the assistance of National Heart Foundation of New Zealand (grant-in-aid number 898) and a grant from the Green Lane Research & Educational Fund.

References

BARR, R. C., and SPACH, M. S. (1978): 'Inverse calculation of QRS-T epicardial potentials from body surface potential distributions for normal and ectopic beats in the intact dog', *Circ. Res.*, **42**, pp. 661–675

BRADLEY, C. P., PULLAN, A. J., and HUNTER, P. J. (1997): 'Geometric modeling of the human torso using cubic Hermite elements', *Ann. Biomed. Eng.*, **25**, pp. 96–111

CHENG, L. K., BODLEY, J. M., and PULLAN, A. J. (2003a): 'Comparison of potential and activation based formulations for the inverse problem of electrocardiology', *IEEE Trans. Biomed. Eng.*, **50**, pp. 11–22

CHENG, L. K., BODLEY, J. M., and PULLAN, A. J. (2003b): 'The effect of experimental and modeling errors on electrocardiographic inverse problems', *IEEE Trans. Biomed. Eng.*, **50**, pp. 23–32

GHANEM, R. N., JIA, C. R. P., and RUDY, Y. (2003): 'Heart-surface reconstruction and ECG electrodes localization using fluoroscopy, epipolar geometry and stereovision: Application to noninvasive imaging of cardiac electric activity', *IEEE Trans. Med. Imag.*, **22**, pp. 1307–1318

GOLDBERGER, E. (1942): 'A simple, indifferent, electrocardiographic electrode of zero potential and a technique of obtaining augmented, unipolar, extremity leads', *Am. Heart J.*, **23**, pp. 483–493

GREENSITE, F., and HUISKAMP, G. (1998): 'An improved method for estimating epicardial potentials from the body surface', *IEEE Trans. Biomed. Eng.*, **45**, pp. 98–104

HANSEN, P. C., and O'LEARY, D. P. (1993): 'The use of the L-curve in the regularization of discrete ill-posed problems', *SIAM J. Sci. Comput.*, **14**, pp. 1487–1503

HUISKAMP, G., and GREENSITE, F. (1997): 'A new method for myocardial activation imaging', *IEEE Trans. Biomed. Eng.*, **44**, pp. 433–446

JOHNSTON, P. R., and GULRAJANI, R. M. (1997): 'A new method for regularization parameter determination in the inverse problem of electrocardiography', *IEEE Trans. Biomed. Eng.*, **44**, pp. 19–39

KASS, M., WITKIN, A., and TERZOPOULOS, D. (1987): 'Snakes: Active contour models', *Int. J. Comput. Vision*, **4**, pp. 321–331

LEGGET, M. E., LEOTTA, D. F., BOLSON, E. L., MCDONALD, J. A., MARTIN, R. W., LI, X.-N., OTTO, C. M., and SHEEHAN, F. H. (1998): 'System for quantitative three-dimensional echocardiography of the left ventricle based on a magnetic-field position and orientation sensing system', *IEEE Trans. Biomed. Eng.*, **45**, pp. 494–504

LU, R. M. T., STEINHAUS, B. M., and DAWSON, A. K. (1992): 'The occurrence of anodal stimulation during bipolar pacing in implantable pacemakers', *in* WERNER, R. (Ed.): 'IEEE Computers in Cardiology' (IEEE Computer Society Press, Los Alamitos, 1992), pp. 495–498

MESSINGER-RAPPORT, B. J., and RUDY, Y. (1998): 'Regularization of the inverse problem in electrocardiography: A model study', *Math. Biosci.*, **89**, pp. 79–118

MESSNARZ, B., SEGER, M., MODRE, R., FISCHER, G., HANSER, F., and TILG, B. (2004): 'A comparison of noninvasive reconstruction of epicardial versus transmembrane potentials in consideration of the space', *IEEE Trans. Biomed. Eng.*, **51**, pp. 1609–1618

MODRE, R., TILG, B., FISCHER, G., and WACH, P. (2002): 'Noninvasive myocardial activation time imaging: A novel inverse algorithm applied to clinical ECG mapping data', *IEEE Trans. Biomed. Eng.*, **49**, pp. 1153–1161

NASH, M. P., BRADLEY, C. P., CHENG, L. K., PULLAN, A. J., and PATERSON, D. J. (2000): 'An experimental-computational framework for validating *in-vivo* ECG inverse methods', *Int. J. Bioelectromagnetism*, **2**

ONNASCH, D. G. W., and PRAUSE, G. P. M. (1992): 'Geometric image correction and iso-center calibration at oblique biplane angiographic views'. IEEE Computers in Cardiology Conf., Durham, NC, IEEE Computer Society Press, Los Alamitos (CA), pp. 647–650

OSTER, H., TACCARDI, B., LUX, R., ERSHLER, P., and RUDY, Y. (1997): 'Noninvasive electrocardiographic imaging. Reconstruction of epicardial potentials, electrograms, and isochrones and localization of single and multiple electrocardiac events', *Circulation*, **96**, pp. 1012–1024

PESOLA, K., NENONEN, J., FENICI, R., LOTJONEN, J., MAKIJARVI, M., FENICI, P., KORHONEN, P., LAUERMA, K., VALKONEN, M., and TOIVONEN, L. (1999): 'Bioelectromagnetic localization of a pacing catheter in the heart', *Phys. Med. Biol.*, **44**, pp. 2565–2578

PULLAN, A. J., CHENG, L. K., NASH, M. P., BRADLEY, C. P., and PATERSON, D. J. (2001): 'Noninvasive electrical imaging of the heart: Theory and model development', *Ann. Biomed. Eng.*, **29**, pp. 817–836

RAMANATHAN, C., GHANEM, R. N., JIA, P., RYU, K., and RUDY, Y. (2004): 'Noninvasive electrocardiographic imaging for cardiac electrophysiology and arrhythmia', *Nat. Med.*, **10**, pp. 422–428

SCHULTE, R. F., SANDS, G. B., SACHSE, F. B., DOSSEL, O., and PULLAN, A. J. (2001): 'Creation of a human heart model and its customisation using ultrasound images', *Biomedizinische Technik*, **46**,

SIPPENSGROENEWEGEN, A., SPEKHORST, H., VAN HEMEL, N. M., KINGMA, J. H., HAUER, R. N. W., DE BAKKER, J. M. T., GRIMBERGEN, C. A., JANSE, M. J., and DUNNING, A. J. (1993): 'Localization of the site of origin of postinfarction ventricular tachycardia by endocardial pace mapping. Body surface mapping compared with the 12-lead electrocardiogram', *Circulation*, **88**, pp. 2290–2306

WALLER, A. D. (1887): 'A demonstration on man of electromotive changes accompanying the heart's beat', *J. Physiol.*, **8**, pp. 229–234

Authors' biographies

Dr LEO CHENG, Dr GREGORY SANDS and Associate-Professor ANDREW PULLAN are members of the Bioengineering Institute at The University of Auckland. Their research interests include constructing computer models of cardiac geometry, structure and electrical function, particularly for use in noninvasively reconstructing electrical activity within the heart.

RENNELLE FRENCH and Dr MALCOLM LEGGET are based at Auckland City Hospital and Dr SELWYN WONG at Middlemore Hospital. They have interests in developing clinical and research uses for three-dimensional echocardiography particularly in valvular heart disease.

STEPHEN WITHY and Dr WARREN SMITH are members of the Green Lane Cardiovascular Service at Auckland City Hospital with particular interest in electrophysiology. Their research interests include the visualisation and treatment of abnormal electrical activity within the heart.